ACS APPLIED MATERIALS & INTERFACES

Research Article

www.acsami.org

Rapid Reversible Superhydrophobicity-to-Superhydrophilicity Transition on Alternating Current Etched Brass

Zhiwei Wang, Liqun Zhu, Weiping Li, and Huicong Liu*

Key Laboratory of Aerospace Materials and Performance (Ministry of Education), School of Materials Science and Engineering, Beihang University, Beijing 100191, China

Supporting Information

ABSTRACT: Reversible surface wetting behavior is a hot topic of research because of the potential engineering applications. In the present work, a hierarchical micro/nanostructure is fabricated on brass by alternate current (AC) etching. The superhydrophilic as-prepared etched brass (EB) turns into superhydrophobic after the modification of stearic acid for 1 min. After annealing at 350 °C for 5 min, the superhydrophobic modified EB surface becomes superhydrophilic again. Furthermore, the annealed EB can restore the superhydrophobicity with the remodification of stearic acid. The wetting transition is realized by stearic acid modification and annealing rapidly in 6 min. The wetting transition mechanism is discussed based on the surface chemical analysis. This method is facile and suitable for the construction of large-scale and complex brass surfaces with tunable wetting behaviors.

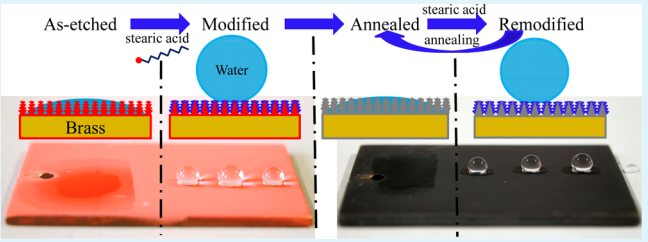

KEYWORDS: *wetting behavior, reversible transition, superhydrophobic, brass, alternating current*

1. INTRODUCTION

Wetting behavior is an important property of a solid surface, which can prolong the service life and extend the application scope of materials. In recent years, superhydrophobic surfaces (with water contact angle (CA) larger than 150°) and superhydrophilic surfaces (with water CA less than 5°) have aroused great interest and been extensively investigated by researchers due to the potential application in self-cleaning materials,[1−3] antifogging surfaces,[4,5] antireflective surfaces,[6,7] microfluid manipulation,[8,9] and so on. Furthermore, reversible wetting behavior such as tunable transition between superhydrophobicity and superhydrophilicity is one of the hot topics of research on developing functional and smart materials in this decade.[10−23] It is known that the chemical composition and microstructure are the key factors influencing the wetting behavior of a solid surface. On one hand, materials which have low surface energy can present hydrophobic property, vice versa, materials with high surface energy are hydrophilic. On the other hand, rough surface can improve the hydrophobicity of hydrophobic materials (has low surface energy) and can also reduce the water CA on the hydrophilic materials (has high surface energy) because of the capillary effect, according to the Wenzel's theory.[24] It is indicated that reversible wetting behavior can be realized through external stimulation to control the chemical composition of solid surface.

Many materials with switchable surface chemical state have been studied to obtain the reversible transition between superhydrophobicity and superhydrophilicity with the response of various stimuli. Jiang and co-workers studied the reversible switching between superhydrophobicity and superhydrophilicity of ZnO films.[10,15] The wetting behaviors of ZnO films were tuned by alternation of UV illumination and dark storage. Other semiconducter oxides such as V_2O_5,[11] WO_x,[16] TiO_2,[17] also present reversible wetting behaviors under UV illumination because of the capability of switching the surface chemical states. In addition, organic surfaces such as azobenzene,[18] poly(N-isopropylacrylamide),[19] polypyrrole[20] and pH-sensitive mixed polymers[21,22] can response to the external stimuli of UV illumination, thermal treatment, electrical potential, and pH, respectively, to change the surface wetting behaviors. Furthermore, reversible wetting transition surfaces on metal substrates such as Ti, Au, and Cu have been investigated.[12,14,22,23,25] However, to the best of our knowledge, little research has been reported on the reversible wetting behavior on brass substrate. Brass is an alloy of Cu and Zn. Because of its good performance, such as low friction, anticorrosion,[26] antimicrobial,[27] and acoustic properties, brass has been widely used in decoration, protection, cooling, structural components, and other fields. With the development of the modern science and technology, the traditional materials need to be multifunctional and more "intelligent". Developing functional surfaces with reversible transition between superhydrophobicity and superhydrophilicity could improve the performance and extend the application scope of brass, providing a good strategy for fabricating smart surfaces with controllable wetting behaviors.

It is known that brass is more stable than copper, so it is hard to fabricate a hierarchical structure on brass using chemical oxidization method used for pure copper.[25] And the reported

Received: January 29, 2013
Accepted: April 29, 2013
Published: April 29, 2013

   dx.doi.org/10.1021/am400299f | ACS Appl. Mater. Interfaces 2013, 5, 4808−4814

method to fabricate superhydrophobic surface on brass usually takes a long time (more than 12 h).[28] In this paper, an alternate current (AC) etching method is used to fabricate hierarchical micro/nanostructure on brass in phosphoric acid solution. The etching duration only needs 5 min. After modification of stearic acid for 1 min, the superhydrophilic as-prepared etched brass (EB) turns into superhydrophobic. After annealing, the superhydrophobic modified EB surface is oxidized and becomes superhydrophilic again. Furthermore, the annealed EB can restore the superhydrophobicity with the remodification of stearic acid. The wetting transition is realized by stearic acid modification and annealing. And the wetting transition cycle is time-saving with the duration of 6 min. This method is facile and suitable for the construction of large-scale and complex brass surfaces with tunable wetting behaviors, which may effectively extend the application scope of brass.

2. EXPERIMENTAL SECTION

2.1. Materials. Acetone, ethanol, phosphoric acid, and stearic acid were of analytical grade and used for experiments reported in the present work. Brass plates (40 mm × 25 mm × 2 mm) containing 64% Cu and 36% Zn were rinsed in acetone and deionized water sequentially before use.

2.1. AC Etching Process. The brass plates were first polished by sandpaper and cleaned by ethanol and deionized water in sequence. And then two pretreated brass plates used as the electrodes were etched in 0.5 M phosphoric acid aqueous solution under an AC voltage of 20 V and 50 Hz. The color of two electrodes turned from golden yellow to red quickly as soon as the AC voltage was applied on brass plates. After certain durations of etching, brass plates were taken out and rinsed by deionized water and ethanol, respectively.

2.2. Reversible Superhydrophobicity-to-Superhydrophilicity Transition. To obtain superhydrophobic surfaces, we immersed the as-prepared EB in 6 mM stearic acid ethanol solution for 1 min. Washed with ethanol and dried at ambient, superhydrophobic surfaces were obtained. The superhydrophobic surface changed to be superhydrophilic by annealing in muffle furnace at 350 °C for 5 min. After annealing, the color of EB turned from red to black. However, the superhydrophobicity can be restored through the remodification with 6 mM stearic acid ethanol solution for 1 min, as previously mentioned. So the reversible transition between superhydrophobicity and superhydrophilicity was realized by the alternation of stearic acid modification and annealing process.

2.3. Characterizations. The scanning electron microscope (SEM) images were obtained using Camscan Apollo 300 (from UK) field-emission SEM after covering a thin film of sputtered platinum on the samples. The surface composition was detected by energy dispersive X-ray spectroscopy (EDX, Oxford Link ISIS from UK) and X-ray photoelectron spectroscopy (XPS, VG Scientific ESCA-Lab 250 from UK) using 200 W Al Kα radiation operating a base pressure $<3 \times 10^{-9}$ mbar. The binding energies were referenced to the C1s line at 284.8 eV from adventitious carbon. X-ray diffraction (XRD) patterns of samples were recorded with a Rigaku D/MAX-RB diffractometer with monochromatized Cu Ka radiation (k = 1.5418). The water CAs were measured using sessile drop method by a contact angle meter (DSA 20, Krüss Instruments GmbH) on five different positions for each surface. The volume of an individual water droplet in all measurements was fixed at 6 μL. The digital photographs of water droplets on surfaces were obtained by a digital camera (Olympus, from Japan).

2.4. Robustness Test. An abrasion test was used to evaluate the robustness of the superhydrophobic surface. As shown in the schematic illustration (see the Supporting Information, Figure S1),[29−31] the sample to be tested faced a nylon wipe, which was served as abrasion surface. A pressure (~2000 Pa) was applied to the sample and the sample was pulled in one direction (the abrasion length was 25 cm) for 10 times. The CAs on the sample were measured after each time of abrasion.

3. RESULTS AND DISCUSSION

Figure 1 presents the morphology of the as-prepared EB with various etching durations. The bare brass surface is smooth

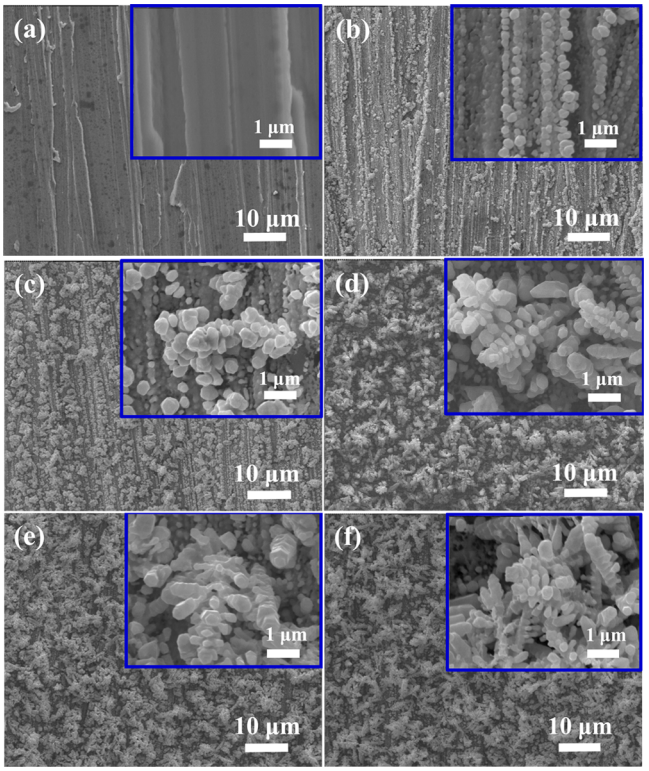

Figure 1. SEM images of the as-prepared EB with various etching durations: (a) 0 min (bare); (b) 45 s; (c) 2.5 min; (d) 5 min; (e) 8 min; (f) 10 min. The insets are high-magnification images.

with clearly scratches due to the mechanical polishing, as shown in Figure 1a. As the etching duration increases to 45 s, it can be seen that nanoparticles with size of hundreds of nanometers grow on the surface and along the scratches (Figure 1b). When the etching duration increases to 2.5 min, the nanoparticles grow larger and aggregate to microbumps, as shown in Figure 1c. After the etching duration increases up to 5 min, as shown in Figure 1d, the brass plate is uniformly and randomly covered with pinecone-like arrays. Each pinecone has a length of several micrometers and is composed of pine nuts which are nano bumps in alignment. Four pine nuts rows grow on every pinecone, forming a 90 angle. Moreover, when the etching duration extends to 8 min, the pinecones and the pine nuts grow larger (Figure 1e). After etching for 10 min, the pinecones aggregate and lie disorderly (Figure 1f). Considering the cost and efficiency, the optimal etching duration is 5 min. In addition, the surface morphologies of EB with various concentrations of phosphoric acid and AC voltages are also investigated (see the Supporting Information, Figures S2 and S3).

Figure 2a_1, b_1, and c_1 show the SEM images of as-prepared EB, modified EB, and annealed modified EB. After etching for 5 min, a hierarchical micro/nanostructure is formed (Figure 2a_1), as discussed above. After the modification of stearic acid ethanol solution for 1 min, as shown in Figure 2b_1, the surface morphology of EB has no apparent change and the modified surface is still composed of pinecone-like arrays. It is indicated that modification of stearic acid for 1 min cannot change the

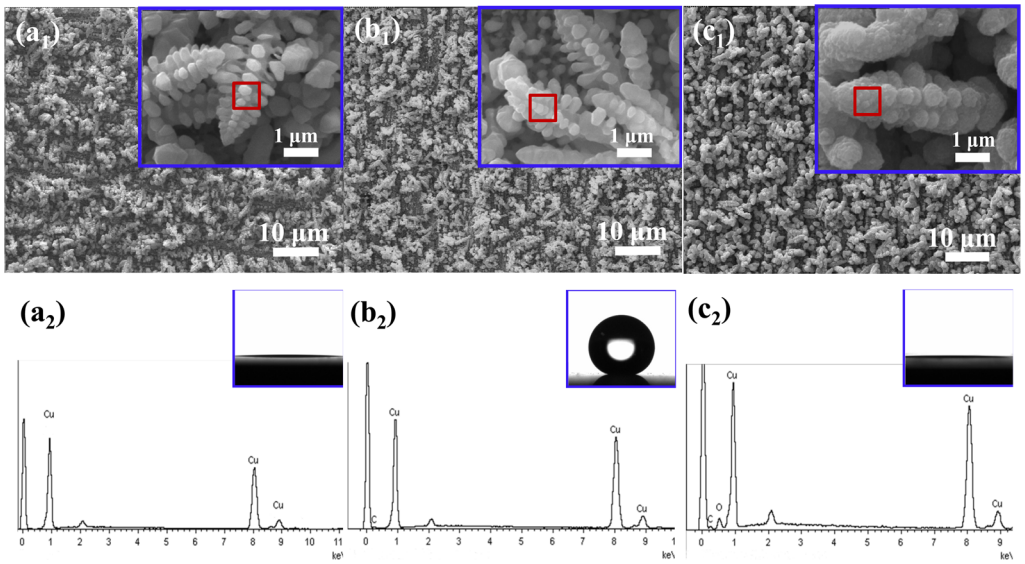

Figure 2. SEM images of (a_1) as-prepared EB; (b_1) stearic acid modified surface of a_1; (c_1) annealed surface of b_1, and the insets are high-magnification images; (a_2, b_2, c_2) EDX spectra corresponding to the red frames in a_1, b_1, and c_1 (the background spectrum is Pt, which has a dispersive peak at 2.1 eV.) The insets correspond to the water CAs on each surface.

surface morphology of EB. However, after annealing in muffle furnace for 5 min, the morphology has been changed compared with modified EB. The pinecone-like arrays become thicker and rougher with nanoscaled wrinkles, which is similar to the observation of Wang and Zhang.[12] The FE-SEM images illustrate that annealing process causes the change of the morphology of EB. To evaluate the surface composition of the three surfaces, the EDX spectra corresponding to the red frames of FE-SEM images have been detected. As is shown in Figure $2a_2$, the pinecones on the EB are composed of Cu only. It means that zinc dissolved selectively and the remained copper forms the hierarchical micro/nanostructure in the etching process. The surface composition of modified EB on the red frame is Cu = 77% and C = 23% in atomic percent (Figure $2b_2$). It is reasonable to deduce that a film containing carbon forms after the modification, however, the morphology of the EB has not changed during the modification. After annealing, the surface composition is Cu = 68%, C = 17%, and O = 15% in atomic percent, as shown in Figure $2c_2$. The emergence of O indicates that copper on the surface has been oxidized by O_2 in annealing process.

In addition, water CAs on the three surfaces were measured and the results are presented in the insets of Figure $2a_2$−c_2. The as-prepared EB is superhydrophilic with the CA less than 5° (Figure $2a_2$). However, the EB gets superhydrophobic property with the CA of 156 ± 1.6° after the modification of stearic acid (Figure $2b_2$). Interestingly, after annealing, the surface transits to superhydrophilicity (CA< 5°) again, as shown in Figure $2c_2$.

Figure 3 shows the XRD patterns of as-prepared EB and annealed EB. The peaks of as-prepared EB at 42.3, 49.3, 72.2, and 87.5° are the diffraction peaks of $Cu_{0.64}Zn_{0.36}$ (JCPDS No. 50−1333), which is from the substrate. The peaks of Cu (JCPDS No. 04−0836) at 43.3, 50.4, and 74.1° indicate that copper concentrates on the substrate after AC etching, which is consistent with the EDX results. However, after annealing, peaks of Cu become unapparent and new peaks appear at 35.5 and 38.7° corresponding to CuO (JCPDS No. 45−0937). Moreover, the peak at 36.4° is assigned to Cu_2O (JCPDS No. 05−0667).

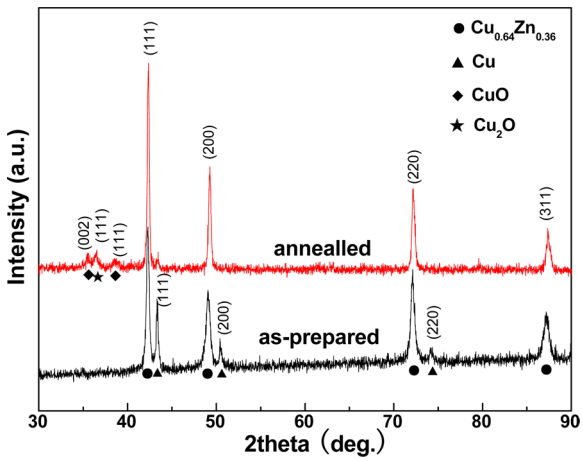

Figure 3. XRD patterns of (a) as-prepared EB and (b) annealed EB.

The superhydrophilic as-prepared EB surface converted into superhydrophobicity with the modification of stearic acid. And the superhydrophobic-modified surface became superhydrophilic after annealing. This transition cycle provides an inspiration to fabricate tunable wetting surfaces. The annealed surface turns out to be superhydrophobic again with no apparent CA decrease after the remodification with stearic acid for 1 min. Thus, we carry out the wetting trasition cycles for several times, the surfaces can be tuned between superhydrophobicity and superhydrophilicity repeatedly. As is shown in Figure 4, the modified surfaces have the water CAs of 155 ± 3.0°, whereas the superhydrophilic surfaces have CAs less than 5°. Moreover, the wetting transition process is rapid, with a duration of 6 min in each cycle.

To further illustrate the wetting behaviors of the modified surface and the annealed surface, we have recorded the contact process between the substrates and water droplet, as shown in Figure 5. As the annealed surface contacts the water droplet, the water spreads rapidly in 0.462 s, presenting superhydrophilic property (Figure 5a−d). However, the remodified surface shows superhydrophobicity with a low water adhesion.

dx.doi.org/10.1021/am400299f | ACS Appl. Mater. Interfaces 2013, 5, 4808−4814

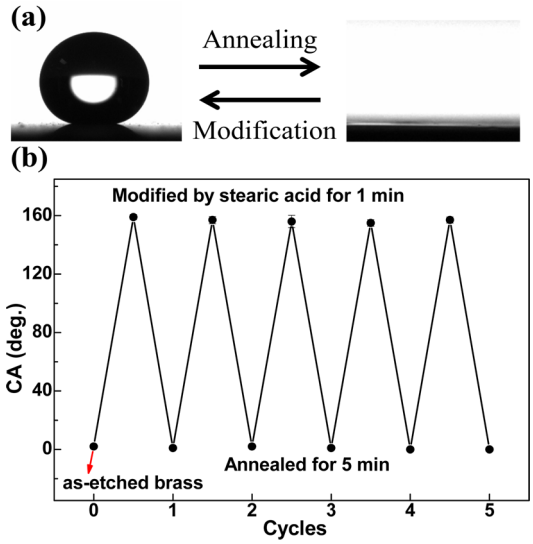

Figure 4. (a) Digital photographs of water droplets on the modified surface and annealed surface; (b) wetting transition cycles on the EB realized by modification and annealing.

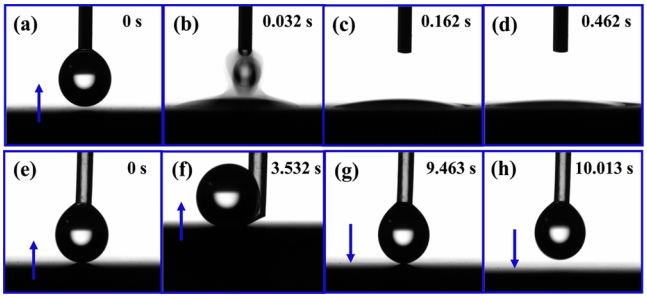

Figure 5. Snapshots of the process of the substrates contact the water droplets: (a–d) the annealed surface; (e, f) the remodified surface. The arrows are the moving direction of the substrates.

The water droplet (6 μL) suspending on the syringe can hardly be pulled down to the surface even when the droplet is squeezed (Figure 5e, f). The annealed surface and the remodified surface presents totally opposite wetting behaviors and the wetting behaviors can be tuned in short time on the same substrate.

In addition, XPS spectra in Figure 6 can further illustrate the surface composition of the modified EB, and the annealed modified EB. The XPS survey spectra indicate that Cu, O and C can be detected on the two surfaces (Figure 6a). The modified EB presents a typical Cu 2p spectrum.[32] However, after annealing, deconvolution of the Cu 2p3/2 presents two peaks centered at 933.9 and 932.5 eV, corresponding to CuO and Cu_2O, respectively,[32−34] which is attributed to the thermal oxidation of Cu after annealing. In Figure 6c, for the modified EB, the O 1s spectrum is resolved into two components centered at 531.7 and 530.6 eV corresponding to chemisorbed oxygen and Cu−O, respectively,[35,36] which demonstrates that Cu−O is introduced after the modification. After annealing, the O 1s spectrum is resolved into two peaks at 529.8 and 530.2 eV, corresponding to CuO and Cu_2O, respectively.[37] The shoulder peak centered at 531.6 eV which is 1.8 eV higher than the main peak of CuO may be attributed to chemisorbed oxygen, according to the research of Robert, Bartel, and Offergeld.[38] The O 1s spectrum of annealed EB further confirms the existence of CuO and Cu_2O after annealing. Furthermore, high resolution spectrum of C 1s of modified EB in Figure 6d has the main peak of C−H or C−C at 284.9 eV and the peak of O−C═O at 288.5 eV,[39] which further illustrate a long-chain aliphatic group containing COO− forms on the modified EB. However, after annealing, the C 1s peak intensity of annealed EB declines obviously, which may be due to the thermal decomposition of long-chain aliphatic group on EB.[40] Table 1 also presents the surface composition of modified EB, annealed EB and remodified EB detected by XPS. It is found that the amount of C reduces from 65.83% to 41.52% after annealing, which implies the decomposition of long-chain aliphatic group. It is consistent with the EDX results in Figure 2. After the remodification with stearic acid, the content of C increases to 51.73%, which indicates that new integral aliphatic group forms on the annealed EB again. The residual carbon indicates that the stearic acid cannot be totally removed after annealing. However, as discussed before, the long-chain aliphatic group has decomposed due to the thermal treatment. And the residual carbon may just adhere to the surface or stay on the surface by physical adsorption. So the residual carbon may not affect the remodification. After the remodification, a new integral long-chain aliphatic group will be introduced on the surface again. And the wetting transition has not been affected after several wetting transition cycles, as shown in Figure 4. Furthermore, the decomposed aliphatic group (residual carbon) might be "washed" away or desorbed in the ethanol solution of stearic acid during the remodification. It may also reduce the effect of residual carbon.

It is well-known that the wettability of the solid surface depends on the surface composition and morphology.[41] To put deep insight into the formation of the micro/nanostructure and the wetting behavior, the mechanisms of AC etching and wetting transition process are discussed, as indicated in Figure 7. As brass plates are immersed in phosphorus acid solution, Zn is preferentially oxidized and the Zn^{2+} are released, which is called "dezincification" because Zn is more active than Cu.[42]The chemical etching process is relatively slow and Cu can gradually dissolve simultaneously with Zn,[43] so it is hard to construct the hierarchical micro/nanostructure. However, AC voltage can facilitate dezincification greatly and then Cu is concentrated on the brass surface, forming a hierarchical micro/nanostructure. As illustrated in Figure 7a, the two brass electrodes serve as the anode and cathode alternately under the AC voltage and the instant electrode reactions are expressed by

$$\text{instant anode: } Zn - 2e^- \leftrightarrow Zn^{2+} \quad (1)$$

$$\text{instant cathode: } 2H^+ + 2e^- \leftrightarrow H_2\uparrow \quad (2)$$

The smooth brass and copper are hydrophilic with the CAs of 85.5 ± 2.2 and 75.0 ± 2.5°, respectively, because the hydroxyl group is absorbed on the metal surfaces (see the Supporting Information, Figure S4a, b). The hierarchical micro/nanostructure of the as-prepared EB surface results in superhydrophilicity because of the 2D and 3D capillary effect (Figure 7b). As the superhydrophilic EB is immersed in the stearic acid ethanol solution, the fresh copper is prone to be oxidized by the dissolved O_2. Then the released Cu^{2+} ions combined $CH_3(CH_2)_{16}COO^-$ ions and form hydrophobic copper stearate ($Cu[CH_3(CH_2)_{16}COO]_2$) on the EB surface[44,45] according to

$$2Cu + O_2 + 4H^+ \leftrightarrow 2Cu^{2+} + 2H_2O \quad (3)$$

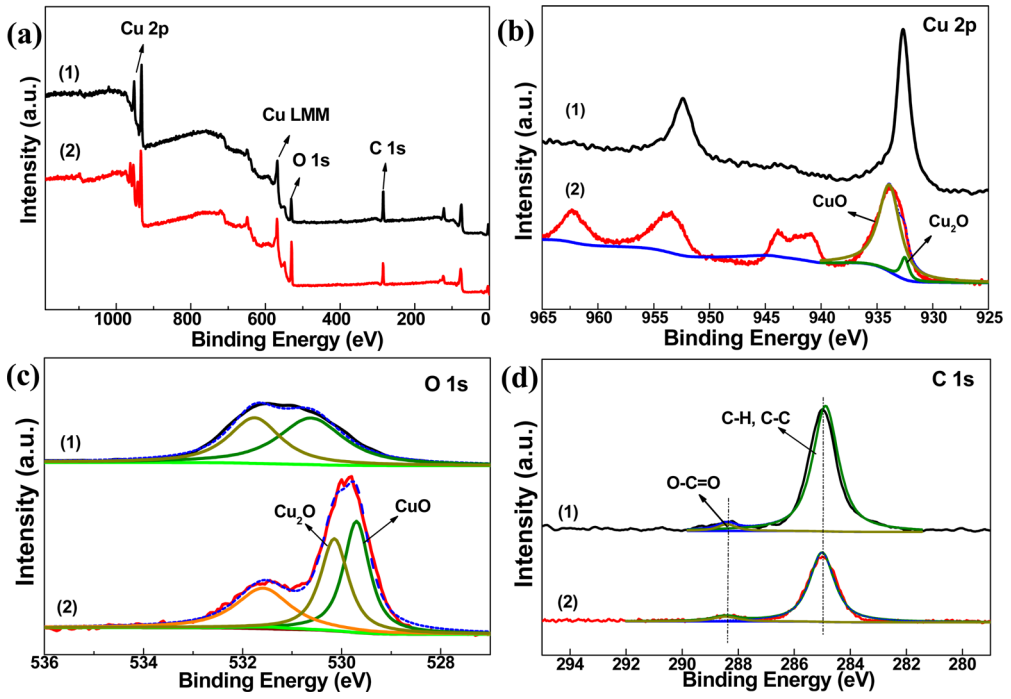

Figure 6. (a) XPS survey spectra and XPS high-resolution spectra of (b) Cu 2p regions, (c) O 1s regions, (d) C 1s regions of (1) modified EB and (2) annealed EB.

Table 1. Surface Atomic Content of C, O, and Cu Detected by XPS on Modified EB, Annealed EB, and Remodified EB after Annealing

at %	C	O	Cu
modified	65.83	20.49	13.68
annealed	41.52	34.85	23.63
remodified	51.73	29.80	18.47

$$Cu^{2+} + CH_3(CH_2)_{16}COO^- \leftrightarrow Cu[CH_3(CH_2)_{16}COO]_2 \quad (4)$$

The modified smooth brass and copper are hydrophobic with the CAs of 96.2 ± 1.4° and 103.3 ± 1.7°, respectively (see the Supporting Information, Figure S4c, d). And as discussed before, the modified EB presents superhydrophobicity with low water adhesion (Figure 5e–h). It is attributed to the low-surface-energy surface ($Cu[CH_3(CH_2)_{16}COO]_2$) and the hierarchical micro/nanostructure of the modified EB. The rough surface can trap a large fraction of air within the hierarchical micro/nanostructure. The trapped air can change the contact state from liquid–solid to liquid–air–solid and prohibit water penetrating the grooves of the surface, leading to high water CA and low water adhesion[46] (Figure 7b_2). During the annealing, as discussed before, the high temperature (350 °C) may break low surface energy group ($CH_3(CH_2)_{16}COO-$) on the surface and eliminate the superhydrophobic property. Meanwhile, Cu is oxidized to Cu_2O or CuO. However, the hierarchical micro/nanostructure is retained although the surface morphology has been changed. The high surface energy CuO/Cu_2O is hydrophilic in air,[47] and the rough hierarchical micro/nanostructure can promote the wetting of water, leading to superhydrophilicity[24] (Figure 7b_3). Similarly, after the annealed EB is immersed in stearic acid solution, a thin film of copper stearate forms on the surface, and then the remodifed EB obtains the superhydrophobicity again (Figure 7b_4). With the modification and annealing proceeding in alternation, the superhydrophobicity-to-superhydrophilicity transition can be realized reversibly with the duration of 6 min. The rapid wetting transition on the hierarchical micro/nanostructure brass can facilitate the potential industrial application.

Robustness is an important property of functional surfaces and it also plays a key role on accessing the applicability of the reversible wetting surfaces. So an abrasion test was carried out to evaluate the robustness of the modified annealed EB (the annealed EB has a more stable surface chemical state than EB) and the results are shown in Figure 8.[29−31] As shown in Figure 8, the CA decreases from 156.4 ± 1.9 to 150.8 ± 2.3° after the first time of abrasion. However, after 6 times of abrasion, the CA decreases to 139.8 ± 1.0°. And then CA decreases slightly and falls to 137.9 ± 1.1° after 10 times of abrasion. The results indicate that the superhydrophobic property is partially lost after the abrasion test. However, the surface still keeps high hydrophobicity with CA higher than 135° after 10 times of abrasion.

To put the research into practical application, the fabrication method must be facile, time-saving, and widely used for large area and complex shape materials. We also fabricated superhydrophobic surfaces on brass using large area brass electrodes (100 mm × 50 mm × 2 mm) with the same parameters as described in the etching progress. As is shown in Figure 9, many water droplets (15–20 μL) present round shapes with large CAs on the modified EB. As an electrochemical method, AC etching is cost-effective, easy to implement, and suitable for large area and complex shape materials, so it is suitable for practical application and production.

4. CONCLUSIONS

In summary, a hierarchical micro/nanostructure on brass substrate is prepared by AC etching method. The superhydrophobic property is obtained with stearic acid modification

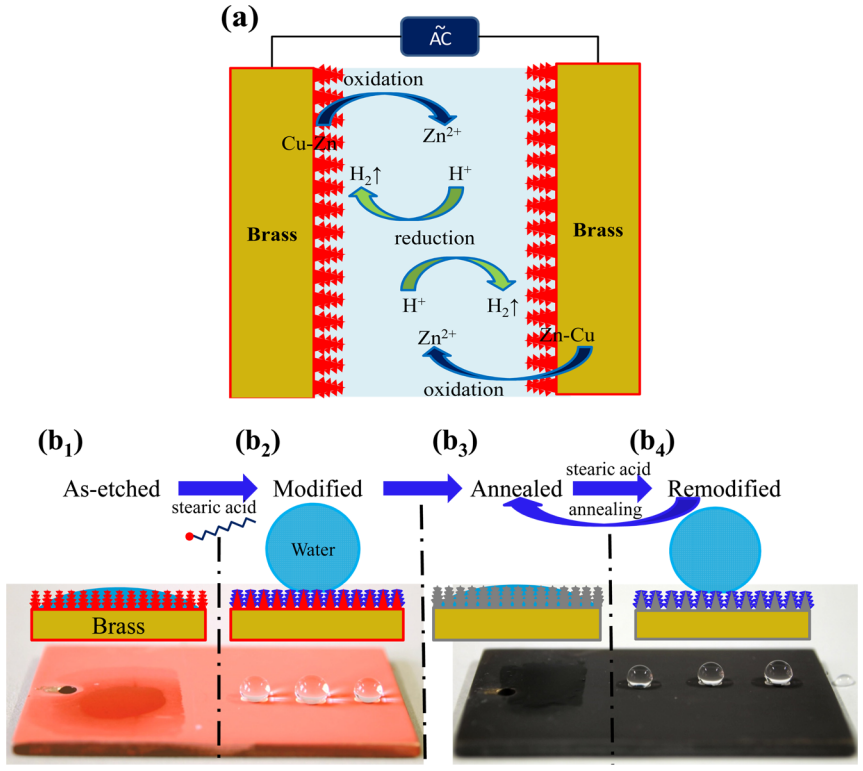

Figure 7. (a) Mechanism of AC etching of brass; (b_1–b_4) the wetting mechanism of surfaces in the experiment process and the corresponding photographs of water droplets on the surfaces.

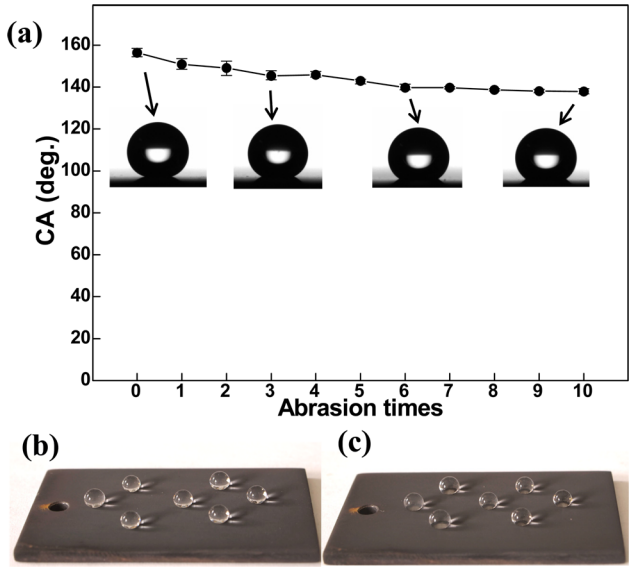

Figure 8. (a) CAs of modified annealed EB after various times of abrasion (the insets are images of water droplets on the same surface before and after 3, 6, and 10 times of abrasion); (b, c) photographs of the surface before and after 10 times of abrasion.

for 1 min. After annealing at 350 °C for 5 min, the superhydrophobic surface turns into superhydrophilicity. As a result, the reversible wetting transition can be realized by stearic acid modification and annealing rapidly within 6 min. This facile and time-saving fabrication approach can be used for constructing large-scale and complex surfaces on brass with tunable wetting behaviors.

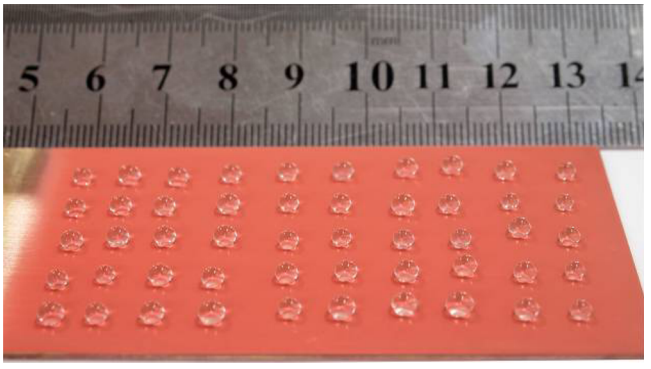

Figure 9. Digital image of large-scale modified EB.

■ ASSOCIATED CONTENT

Supporting Information

Schematic illustration of the abrasion test to evaluate the robustness of the modified annealed EB. SEM images of etched brass with various concentrations of phosphoric acid and AC voltages. Images of water droplets on the smooth brass, smooth copper, modified smooth brass, and modified smooth copper. This material is available free of charge via the Internet at http://pubs.acs.org./

■ AUTHOR INFORMATION

Corresponding Author

*E-mail: liuhc@buaa.edu.cn (H.L.). Tel: +86 1082317113. Fax: +86 1082317133.

Notes

The authors declare no competing financial interest.

■ ACKNOWLEDGMENTS

The authors are very grateful for the support from the National Natural Science Foundation of China (Grant No. 51071012).

■ REFERENCES

(1) Blossey, R. *Nature* **2003**, *2*, 301−306.
(2) Bhushan, B.; Jung, Y. C.; Koch, K. *Langmuir* **2009**, *25*, 3240−3248.
(3) Anandan, S.; Narasinga Rao, T.; Sathish, M.; Rangappa, D.; Honma, I.; Miyauchi, M. *ACS Appl. Mater. Interfaces* **2012**, *5*, 207−212.
(4) Hong, X.; Gao, X.; Jiang, L. *J. Am. Chem. Soc.* **2007**, *129*, 1478−1479.
(5) Introzzi, L.; Fuentes-Alventosa, J. M.; Cozzolino, C. A.; Trabattoni, S.; Tavazzi, S.; Bianchi, C. L.; Schiraldi, A.; Piergiovanni, L.; Farris, S. *ACS Appl. Mater. Interfaces* **2012**, *4*, 3692−3700.
(6) Zhang, X.; Sato, O.; Taguchi, M.; Einaga, Y.; Murakami, T.; Fujishima, A. *Chem. Mater.* **2005**, *17*, 696−700.
(7) Li, X.; Du, X.; He, J. *Langmuir* **2010**, *26*, 13528−13534.
(8) Cheng, Z.; Lai, H.; Zhang, N.; Sun, K.; Jiang, L. J. *Phys. Chem. C* **2012**, *116*, 18796−18802.
(9) Kobayashi, T.; Shimizu, K.; Kaizuma, Y.; Konishi, S. *Lab Chip* **2010**, *11*, 639−644.
(10) Feng, X. J.; Feng, L.; Jin, M. H.; Zhai, J.; Jiang, L.; Zhu, D. B. *J. Am. Chem. Soc.* **2004**, *126*, 62−63.
(11) Lim, H. S.; Kwak, D.; Lee, D. Y.; Lee, S. G.; Cho, K. *J. Am. Chem. Soc.* **2007**, *129*, 4128−4129.
(12) Wang, G.; Zhang, T. *ACS Appl. Mater. Interfaces* **2011**, *4*, 273−279.
(13) Chaudhary, A.; Barshilia, H. C. *J. Phys. Chem. C* **2011**, *115*, 18213−18220.
(14) Wang, D.; Wang, X.; Liu, X.; Zhou, F. *J. Phys. Chem. C* **2010**, *114*, 9938−9944.
(15) Liu, H.; Feng, L.; Zhai, J.; Jiang, L.; Zhu, D. *Langmuir* **2004**, *20*, 5659−5661.
(16) Kwak, G.; Lee, M.; Yong, K. *Langmuir* **2010**, *26*, 9964−9967.
(17) Feng, X.; Zhai, J.; Jiang, L. *Angew. Chem., Int. Ed.* **2005**, *44*, 5115−5118.
(18) Lim, H. S.; Han, J. T.; Kwak, D.; Jin, M.; Cho, K. *J. Am. Chem. Soc.* **2006**, *128*, 14458−14459.
(19) Sun, T.; Wang, G.; Feng, L.; Liu, B.; Ma, Y.; Jiang, L.; Zhu, D. *Angew. Chem.* **2004**, *116*, 361−364.
(20) Xu, L.; Chen, W.; Mulchandani, A.; Yan, Y. *Angew. Chem., Int. Ed.* **2005**, *44*, 6009−6012.
(21) Yu, X.; Wang, Z.; Jiang, Y.; Shi, F.; Zhang, X. *Adv. Mater.* **2005**, *17*, 1289−1293.
(22) Jiang, Y.; Wang, Z.; Yu, X.; Shi, F.; Xu, H.; Zhang, X.; Smet, M.; Dehaen, W. *Langmuir* **2005**, *21*, 1986−1990.
(23) Wan, P.; Jiang, Y.; Wang, Y.; Wang, Z.; Zhang, X. *Chem. Commun.* **2008**, *0*, 5710−5712.
(24) Wenzel, R. N. *Ind. Eng. Chem.* **1936**, *28*, 988−994.
(25) Zhu, X.; Zhang, Z.; Men, X.; Yang, J.; Xu, X. *ACS Appl. Mater. Interfaces* **2010**, *2*, 3636−3641.
(26) Goidanich, S.; Brunk, J.; Herting, G.; Arenas, M. A.; Odnevall Wallinder, I. *Sci. Total Environ.* **2011**, *412*−*413*, 46−57.
(27) Zhu, L.; Elguindi, J.; Rensing, C.; Ravishankar, S. *Food Microbiol.* **2012**, *30*, 303−310.
(28) Wu, W.; Chen, M.; Liang, S.; Wang, X.; Chen, J.; Zhou, F. *J. Colloid Interface Sci.* **2008**, *326*, 478−482.
(29) Liu, L.; Zhao, J.; Zhang, Y.; Zhao, F.; Zhang, Y. *J. Colloid Interface Sci.* **2011**, *358*, 277−283.
(30) Liu, L.; Xu, F.; Yu, Z.; Dong, P. *Appl. Surf. Sci.* **2012**, *258*, 8928−8933.
(31) Fei-Yan, X. U.; Li-Jun, L.; Jian, Q.; Bei, L.; Shuang, M. *Acta Phys-Chim. Sin.* **2012**, *28*, 693−698.
(32) Wanger, C. D.; Riggs, W. M.; Davis, L. E.; Moulder, J. F.; Muilenberg, G. E. *Handbook of X Ray Photoelectron Spectroscopy*; Perkin-Elmer: Eden Prairie, MN, 1979, p 82.
(33) Liu, L.; Xu, F.; Ma, L. *J. Phys. Chem. C* **2012**, *116*, 18722−18727.
(34) She, Z.; Li, Q.; Wang, Z.; Li, L.; Chen, F.; Zhou, J. *ACS Appl. Mater. Interfaces* **2012**, *4*, 4348−4356.
(35) Xu, T.; Yang, S.; Lu, J.; Xue, Q.; Li, J.; Guo, W.; Sun, Y. *Diam. Relat. Mater.* **2001**, *10*, 1441−1447.
(36) Tang, K.; Wang, X.; Yan, W.; Yu, J.; Xu, R. *J. Membr. Sci.* **2006**, *286*, 279−284.
(37) Ghijsen, J.; Tjeng, L. H.; van Elp, J.; Eskes, H.; Westerink, J.; Sawatzky, G. A.; Czyzyk, M. T. *Phys. Rev. B* **1988**, *38*, 11322−11330.
(38) Robert, T.; Bartel, M.; Offergeld, G. *Surf. Sci.* **1972**, *33*, 123−130.
(39) Zhu, X.; Zhang, Z.; Men, X.; Yang, J.; Xu, X.; Zhou, X. *Appl. Surf. Sci.* **2011**, *257*, 3753−3757.
(40) Jaw, K.; Hsu, C.; Lee, J. *Thermochim. Acta* **2001**, *367*−*368*, 165−168.
(41) Lafuma, A.; Quere, D. *Nature* **2003**, *2*, 457−460.
(42) Stillwell, C. W.; Turnipseed, E. S. *Ind. Eng. Chem.* **1934**, *26*, 740−743.
(43) Joseph, G.; Arce, M. T. *Corros. Sci.* **1967**, *7*, 597−605.
(44) Wang, S.; Feng, L.; Jiang, L. *Adv. Mater.* **2006**, *18*, 767−770.
(45) Huang, Y.; Sarkar, D. K.; Chen, X. G. *Mater. Lett.* **2010**, *64*, 2722−2724.
(46) Cassie, A. B. D.; Baxter, S. *Trans. Faraday Soc.* **1944**, *40*, 546−551.
(47) Liu, X.; Zhou, J.; Xue, Z.; Gao, J.; Meng, J.; Wang, S.; Jiang, L. *Adv. Mater.* **2012**, *24*, 3401−3405.